SYNTHESIS AND CHARACTERIZATION OF ZNO/CUS NANOCOMPOSITE FOR PHOTOCATALYTIC WASTEWATER DECONTAMINATION

Ahmed Fawzy [(1)]; Reem Mohamed [(2)];, Hany A. Elazab[(3)]; Mohammed E. M. Ali [(4)]; M. Mohsen[(2)]

1) Faculty of Graduate Studies and Environmental Research, Ain Shams University, Cairo, Egypt 2) Physics Department, Faculty of Science, Ain Shams University, Cairo, Egypt 3) Chemical and Biochemical Engineering Department, Missouri University of Science and Technology, Rolla, MO 65409, USA. 4) Water Pollution Research Department, National Research Center, Cairo, Egypt.

ABSTRACT

This study presents the synthesis and characterization of ZnO/CuS hybrid nanocomposites designed for the photocatalytic degradation of methylene blue dye. The nanocomposites were synthesized using a microwave-assisted hydrothermal method, where copper sulfide (CuS) was prepared first, followed by the addition of zinc oxide nanoparticles (ZnO NPs). The successful integration of CuS and ZnO was confirmed using various characterization techniques, including X-ray diffraction (XRD), transmission electron microscopy (TEM), scanning electron microscopy (SEM), energy dispersive X-ray (EDX) spectroscopy, and Fourier-transform infrared spectroscopy (FTIR). Optical properties were also investigated utilizing diffused reflectance spectroscopy (DRS), revealing that the band gap energy of the hybrid material (3.21 eV) was lower than that of pure ZnO (3.29 eV), indicating enhanced photocatalytic activity. Photocatalytic degradation experiments demonstrated high efficiency in decolorizing methylene blue, with complete dye degradation achieved under optimal conditions: photocatalyst dosage of 0.1 g/L, dye concentration of 10 ppm, and pH of 9. These findings highlight the potential of ZnO/CuS nanocomposites for practical applications in wastewater treatment. Furthermore, the influence of salinity, inorganic oxyanions, and scavengers on photocatalytic performance was systematically investigated, providing important insights into the operational parameters required to utilize ZnO/CuS nanocomposites in environmental remediation effectively.

Keywords: microwave; hydrothermal; wastewater; ZnO; CuS; photocatalysis

INTRODUCTION

The global water crisis, exacerbated by industrial pollution and rapid urbanization, is one of the most pressing environmental issues of the 21st century (**Schwarzenbach et al., 2010**). Wastewater contaminated with persistent organic pollutants (POPs), heavy metals, and emerging contaminants poses significant risks to both aquatic ecosystems and public health

Vol. (54); No. (4); Apr. 2025
Print ISSN 1110-0826
Online ISSN 2636 - 3178

(da Costa Filho et al., 2022; Offiong et al., 2019). Annually, approximately 10,000 different commercial dyes and pigments are produced worldwide, with 10-15% of this total being lost in effluent during the dyeing process. Methylene blue, commonly used in industries such as textiles, paper manufacturing, rubber, plastics, leather, cosmetics, and food processing, is a prime example. Even at low concentrations, its presence in industrial effluent is highly visible. When left untreated, these colored wastewaters increase the chemical oxygen demand and enhance toxicity in water bodies. Therefore, it is essential to remove synthetic dyes from wastewater before discharge into the environment to safeguard public health and preserve the ecological balance (**Amar et al., 2022; Mohammed et al., 2014**).

Conventional water treatment methods, such as adsorption, biological processes, membrane bioreactors, electrochemical treatment, nanofiltration, coagulation/flocculation, chemical oxidation, ozonation, and membrane processes, have proven to be largely inefficient for removing recalcitrant pollutants. As a result, there is a pressing need for the development of new and more effective technologies for water and wastewater treatment **(Crini and Lichtfouse, 2019; Khader et al., 2024; Plumlee et al., 2008**).

Advanced Oxidation Processes (AOPs) are emerging as powerful and efficient techniques for wastewater treatment, particularly for the degradation of persistent organic pollutants and the elimination of pathogenic microorganisms. AOPs rely on the generation of highly reactive oxygen species (ROS), such as hydroxyl radicals ($^{\bullet}OH$), which are capable of breaking down complex and recalcitrant organic contaminants into simpler, less harmful compounds **(Hoffmann et al., 1995**). These processes offer a significant advantage due to their ability to achieve near-complete mineralization of pollutants, converting them into harmless end-products like carbon dioxide (CO_2) and water (H_2 O).

Among the different types of AOPs, photocatalysis has emerged as one of the most promising and widely studied approaches. In photocatalytic AOPs, semiconductor photocatalysts such as titanium dioxide (TiO_2), zinc oxide (ZnO), and zirconium dioxide (ZrO_2) are activated under light irradiation of suitable energy (**Guo et al., 2012**). This irradiation excites electrons from the valence band to the conduction band of the

semiconductor, generating electron-hole pairs. These electron-hole pairs interact with water and dissolved oxygen to produce reactive oxygen species (ROS), including hydroxyl radicals (•*OH*) and superoxide ions (O_2^{-}•). These species play a critical role in oxidizing organic pollutants, often leading to their complete mineralization into non-toxic products (**Capelo-Martınez et al., 2004; Lu et al., 2016**). The primary advantages of photocatalytic AOPs include their ability to operate under ambient temperature and pressure conditions and their high efficiency in achieving complete degradation of pollutants. Moreover, using solar energy as a sustainable light source further enhances photocatalytic processes' economic feasibility and environmental friendliness, making them a promising solution for wastewater purification (**Khader et al., 2024**).

Among the diverse range of photocatalytic materials, ZnO has garnered significant attention due to its excellent photocatalytic activity, non-toxicity, accessibility, and low-cost **(Lee et al., 2016**). ZnO possesses a wide bandgap of 3.37 eV and a high exciton binding energy of 60 meV at room temperature, making it highly effective as a photocatalyst under UV radiation **(Ozgur, 2005**). These properties enable ZnO to generate electron-hole pairs upon photoexcitation, which then interact with water and dissolved oxygen to produce reactive oxygen species (ROS) such as hydroxyl radicals (•*OH*), capable of degrading organic pollutants. However, the practical application of ZnO in photocatalytic degradation is limited by several challenges. First, its wide bandgap restricts light absorption to the ultraviolet region, which accounts for only about 4% of the solar spectrum. This severely reduces its ability to utilize visible light, limiting its energy efficiency. Second, ZnO suffers from a high recombination rate of photogenerated electron-hole pairs, which significantly reduces its quantum efficiency and overall photocatalytic performance(**Leidinger et al., 2012**). Additionally, its small specific surface area further hampers mass transfer, making it less effective for large-scale applications. Despite these limitations, efforts to enhance ZnO's photocatalytic efficiency such as surface modification, doping with metals or non-metals, and forming nanocomposites with other materials are ongoing, aiming to broaden its applicability in the degradation of organic pollutants in wastewater **(Kumar and Rao, 2015**).

Vol. (54); No. (4); Apr. 2025
Print ISSN 1110-0826
Online ISSN 2636 - 3178

Doping, surface modification, and heterojunction formation with other semiconductors are widely studied strategies to enhance the photocatalytic performance of ZnO (**Hezam et al., 2017**). One effective approach is the preparation of nanocomposites by combining ZnO with narrow-bandgap semiconductors, which improves visible light absorption and charge separation (**Low et al., 2017**). In this context, CuS has emerged as a promising candidate for forming heterojunctions with ZnO due to its unique properties (**Regulacio and Han, 2010**). CuS is a p-type semiconductor with a narrow bandgap ranging from 1.2 to 2.0 eV, depending on its stoichiometric composition and crystalline structure (**Zhao and Burda, 2012**). Incorporating CuS into ZnO nanostructures offers several advantages: extended light absorption into the visible spectrum enhances solar energy utilization, while the formation of a p-n junction at the ZnO/CuS interface facilitates efficient charge separation, reducing the recombination rate of photogenerated electron-hole pairs. Additionally, the increased surface area and availability of active sites improve pollutant adsorption and degradation (**Lin et al., 2023; Pan et al., 2020**). Moreover, CuS nanoparticles exhibit near-infrared plasmonic behavior, which enhances local electric fields, further boosting the photocatalytic performance of ZnO/CuS nanocomposites (**Reem Mohammed et al., 2022; Zhao et al., 2009**). These synergistic effects make CuS an excellent choice for coupling with ZnO to achieve superior photocatalytic efficiency. Among the various ZnO-based heterostructures, ZnO/CuS nanocomposites have demonstrated exceptional potential for pollutant degradation (**Yendrapati et al., 2020**). Their enhanced photocatalytic activity is primarily attributed to the favorable band alignment between the two semiconductors. Specifically, the conduction band of CuS is more negatively positioned than that of ZnO, while the valence band of ZnO is more positively positioned than CuS (**Mohammed. R et al., 2022**). This alignment promotes efficient separation and transport of photogenerated charge carriers, effectively reducing recombination and improving overall photocatalytic performance **(Basu et al., 2014; Sudhaik, Raizada, Rangabhashiyam, Singh, Nguyen, Van Le, Khan, Hu, Huang, Ahamad, et al., 2022**).

Vol. (54); No. (4); Apr. 2025
Print ISSN 1110-0826
Online ISSN 2636 - 3178

To date, relatively few studies have focused on combining ZnO and CuS nanoparticles to synthesize CuS@ZnO nanocomposites **(Gao et al., 2023; M. D. Khan et al., 2022; Reem Mohammed et al., 2022; Ning et al., 2023; Pang et al., 2022; Sudhaik, Raizada, Rangabhashiyam, Singh, Nguyen, Van Le, Khan, Hu, Huang,** and **Ahamad, 2022; Zhu et al., 2022**). Among these, several investigations have explored the fabrication of ZnO nanorods decorated with CuS quantum dots for the photocatalytic decontamination of wastewater, specifically targeting organic pollutants through advanced oxidation processes **(Gao et al., 2023; Reem Mohammed et al., 2022; Zhang et al., 2015**). In related work, Pang et al. developed porous ZnO structures integrated with CuS quantum dots, which were effectively employed for gas purification applications, particularly in the removal of SO_3 and Hg ions (**Pang et al., 2022**). Similarly, Ning et al. synthesized ZnO/CuS piezo-catalysts using a solid-state grinding method. These catalysts demonstrated remarkable efficiency in the photodegradation of methylene blue dye and the reduction of N_2 to ammonia, achieving a performance that was four times greater than that of pristine ZnO (**Ning et al., 2023**). These findings emphasize the versatility and potential of CuS@ZnO nanocomposites for diverse applications, including wastewater treatment, gas purification, and photocatalytic reactions. This study developed ZnO/CuS nanocomposites via a three-step microwave hydrothermal method for wastewater pollutant degradation. The nanocomposites were characterized using techniques such as DRS, TEM, SEM-EDX, and FT-IR. Their photocatalytic performance was evaluated using methylene blue as a model pollutant under simulated solar light, with a systematic investigation of the effects of catalyst loading, pollutant concentration, pH, and ionic strength. The recyclability of the photocatalyst was also evaluated through multiple degradation cycles.

Vol. (54); No. (4); Apr. 2025
Print ISSN 1110-0826
Online ISSN 2636 - 3178

EXPERIMENTAL SECTION

Materials: Zinc acetate dihydrate (Zn $(CH_3COO)_2.2H_2O$), and hexamethylenetetramine (HMT), are supplied by Merck Chemicals Company, Germany. Copper acetate monohydrate CA (Cu $(CH_3COO)_2$. H_2O, ≥ 99.0 %), is supplied by Sigma Aldrich, Germany. Thiourea TU (CH_4N_2S) is supplied by Fluka Chemicals Company, Germany. All the chemicals employed are of analytical grade and are applied without further purification. The solvent used in all experimental procedures is deionized water. As well as reagent grade methylene blue (MB) is supplied by LOBA Chemie.

METHODOLOGY

Preparation of copper sulfide quantum dotes (CuS) The CuS was synthesized by the microwave hydrothermal method as previously reported (Nafees et al., 2012; Nethravathi et al., 2019; Santos et al., 2020; Tadjarodi and Khaledi, 2010). In short, 10.5 mmol or 1.9 g of copper acetate monohydrate [$Cu(CH_3COO)_2 \cdot H_2O$] was dissolved in 50 mL of DI water to form a transparent blue solution. Simultaneously, 4 g of thiourea (TU) was dissolved into 50 mL DI water. Consequently, both solutions were then ultrasonicated for 90 seconds to get them completely dissolved. Right after the addition, the solution's color changed to greyish brown. Followed by extra mixing for 40 minutes to become homogeneous. The thus prepared solution was transferred into a microwave reactor (1000 W, 200 °C) for cyclic heating: a cycle consisting of 2 min of microwave irradiation at 50% of full power, 500 W, followed by 30 seconds of cooling; this was done three times. The produced black precipitate, believed to be CuS quantum dots, was then collected and rinsed with deionized water. Finally, it was then put into an oven at 60 °C for 6 h for oven-drying before characterization.

Preparation of Zinc oxide nanoparticles (ZnO NPs): ZnO nanostructures were synthesized via a microwave-assisted hydrothermal method as reported previously (Barreto et al., 2013; Boudjadar et al., 2010; Gerbreders et al., 2020; Ghai et al., 2020; Mahpeykar et al., 2012) with slight modification. In a typical procedure, 2.195 g (10 mmol) of zinc acetate dihydrate [$Zn(CH_3COO)_2 \cdot 2H_2O$] was dissolved in 100 mL of deionized water (DI) to form a

clear solution. Subsequently, 1.42 g (10 mmol) of hexamethylenetetramine (HMT) was added to the zinc acetate solution. The mixture was subjected to ultrasonication for 30 min to ensure complete dissolution and homogenization, resulting in a white suspension. The prepared suspension was transferred to a microwave oven (1000 W, 200 °C) and subjected to a cyclic heating process. Each cycle consisted of 2 min of microwave irradiation followed by a 30 s cooling period, repeated three times. The resulting white precipitate, presumed to be ZnO nanostructures, was collected and washed thoroughly with DI water. The product was then dried in an oven at 60 °C for 6 h before further characterization.

Fabrication of CuS/ZnO nanocomposite: The CuS/ZnO nanocomposite photocatalysts were synthesized using a combined ultrasonic-microwave hydrothermal approach. Initially, 0.1 g of pre-synthesized CuS was dispersed in 100 mL of deionized (DI) water, sonicated for 30 minutes, and subsequently magnetically stirred for another 30 minutes. Simultaneously, 2 g of pre-synthesized ZnO nanostructures were dissolved in a separate DI water solution and stirred for 30 minutes. The two dispersions CuS quantum dots (QDs) and ZnO nanostructures were then mixed thoroughly and subjected to vigorous stirring at 250 °C for 30 minutes. Following this, the reaction mixture was transferred to a 100 mL beaker and subjected to microwave hydrothermal synthesis. The process involved five cycles, with each cycle comprising 2 minutes of microwave irradiation. The resulting grey precipitate, identified as CuS/ZnO nanocomposites, was collected through vacuum filtration and washed several times with DI water to remove residual impurities. Finally, the product was oven-dried at 70 °C for 10 hours in preparation for further characterization.

Vol. (54); No. (4); Apr. 2025
Print ISSN 1110-0826
Online ISSN 2636 - 3178

Characterization: The optical properties have been obtained via diffused reflectance spectroscopy (DRS) JASCO. V-570 Spectrophotometer. The morphological structure (i.e., size and shape) of the as-prepared CuS/ZnO nanocomposites was investigated using a transmission electron microscope (TEM) JEOL JEM-2100F operated at an operating voltage of 200 kV. Furthermore, the surface morphology/texture was investigated using a scanning electron microscope equipped with energy dispersive spectroscopy (SEM-EDS, QUANTA FEG250) with an operating voltage of 20 kV. The crystallographic structure of CuS/ZnO nanocomposites investigated via X-ray diffraction (XRD) analysis were recorded using a D8 Discover X-ray diffractometer (Bruker, Karlsruhe, Germany) by employing Cu-Kα source (λ = 1.5418 Å). The diffractometer was set up at the generator voltage of 40 kV with a current of 30 mA. Different diffraction patterns were obtained within the 2θ range of 0 to 80 degrees with a scan rate of 0.5°/min. FTIR spectra were determined with a JASCO 6700 FT-IR spectrometer at the range of 4000–400 cm^{-1} (JASCO, UK).

Photocatalytic activity measurements: The photocatalytic activity of CuS/ZnO nanocomposites was systematically evaluated to determine the impact of various experimental conditions on the degradation efficiency of methylene blue (MB) dye under simulated sunlight. Optimization studies were conducted by varying the following parameters: photocatalyst dosage (0.2–1 g/L), dye concentration (10–40 ppm), pH levels (3–11), salinity (0.25%–2.5% NaCl), and the presence of scavengers. The photodegradation efficiency was quantified using UV-Vis spectrophotometry. Aliquots of the sample solution were collected at 15-minute intervals. The collected suspensions were filtered using syringe filters (Whatman, 0.45 µm) to remove residual photocatalyst particles. The concentrations of MB at different time points were measured with a UV-Vis spectrophotometer (JASCO V-730).

The photocatalytic degradation efficiency was calculated using the following equations:

$$Degradation\ \% = \frac{C_0 - C_t}{C_0} \times 100 \qquad (3)$$

where C_0 and C_t are the concentrations of the waste before and after different irradiation times, respectively.

Vol. (54); No. (4); Apr. 2025
Print ISSN 1110-0826
Online ISSN 2636 - 3178

RESULTS

Effect of Photocatalyst Dose: The degradation efficiency of MB dye under simulated sunlight conditions was investigated as a function of the CuS/ZnO nanocomposite dose (0.2–1 g/L) using a MB dye solution with 10 ppm concentration at pH 6.5. The results, depicted in Fig. 1, reveal a significant enhancement in photodegradation efficiency with an increase in catalyst dosage.

At a dose of 1 g/L, the photodegradation efficiency reached its maximum, achieving nearly 99% degradation within 45 minutes. When the dosage was reduced to 0.5 g/L, the degradation efficiency decreased to approximately 60% in 45 minutes. Further reductions in catalyst dosage to 0.4, 0.3, and 0.2 g/L resulted in progressively lower degradation efficiencies, with minimal activity observed at 0.2 g/L.

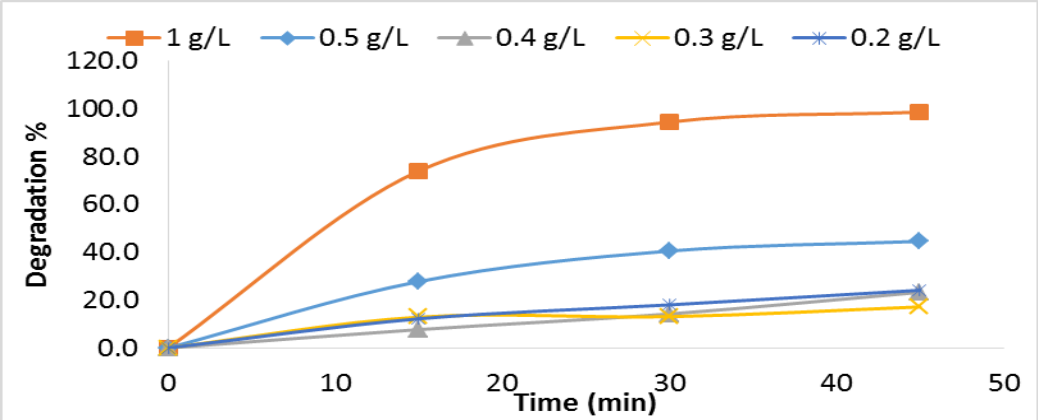

Fig. 1. Effect of CuS/ZnO Photocatalyst Dose on the Photodegradation Efficiency of MB Dye

Vol. (54); No. (4); Apr. 2025
Print ISSN 1110-0826
Online ISSN 2636 - 3178

Effect of Dye Concentration: The photocatalytic activity of the CuS/ZnO nanocomposite was evaluated by studying the degradation of MB dye under varying initial concentrations, ranging from 10 to 40 ppm and illustrated in Fig. 2. The experiments were conducted under optimized conditions, with a catalyst dose of 1 g/L and an initial pH of 6.5 after 45 minutes of irradiation. The degradation efficiency showed a clear dependency on the dye concentration, with higher efficiencies observed at lower MB concentrations. At 10 ppm, the degradation efficiency reached approximately 98% within 30 minutes. As the MB concentration increased to 20 ppm, the degradation efficiency decreased to about 85% in 60 minutes. Further increases in MB concentration to 30 and 40 ppm resulted in significantly reduced degradation efficiencies of around 60% and 40%, respectively, even after 60 minutes. At these higher concentrations, the light absorption by MB molecules competes with the photocatalyst.

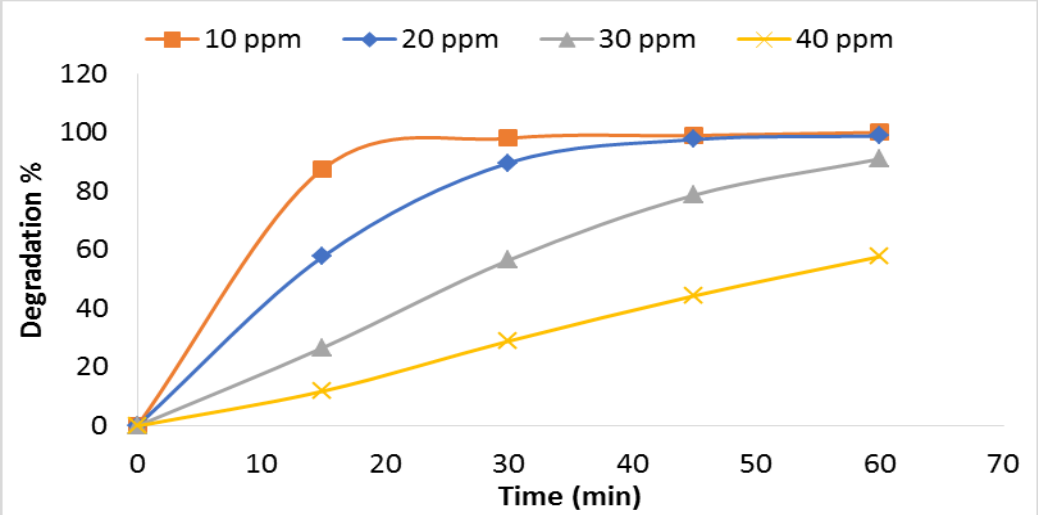

Fig. 2. Effect MB Dye Concentration on the photocatalytic activity of CuS/ZnO Photocatalyst on the Photodegradation Efficiency MB Dye.

Vol. (54); No. (4); Apr. 2025
Print ISSN 1110-0826
Online ISSN 2636 - 3178

Effect of pH: The pH plays a pivotal role in the photocatalytic degradation of methylene blue (MB) dye, as it significantly influences the properties of the dye molecules and the surface charge characteristics of the CuS/ZnO nanocomposite. The effect of pH was investigated using an initial MB concentration of 10 ppm, with a catalyst dose of 1 g/L. Adjusting the pH significantly alters surface interactions and adsorption processes, which in turn impact the overall photocatalytic performance. To investigate this effect, the degradation efficiency was evaluated across a broad pH range (3, 5, 9, and 11), as depicted in Fig. 3.

At pH 3, the photocatalytic system demonstrated degradation and adsorption efficiencies ranging between 85% and 100% within 15–30 minutes. Similarly, at pH 5, the system achieved comparable degradation efficiencies of 86% to 100% over the same time interval. Notably, at pH 9, the performance improved further, with degradation efficiencies reaching 91% to 100% in 15–30 minutes, accompanied by robust adsorption. Finally, at pH 11, the system achieved complete degradation efficiency, with 100% removal observed.

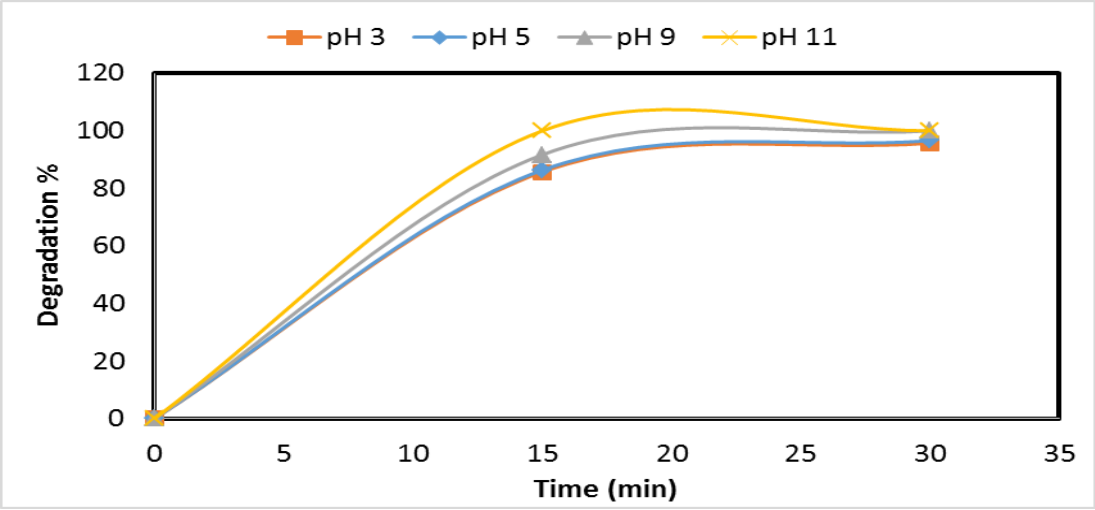

Fig. 3. Effect pH on the photocatalytic activity of CuS/ZnO Photocatalyst on the Photodegradation Efficiency MB Dye

Vol. (54); No. (4); Apr. 2025
Print ISSN 1110-0826
Online ISSN 2636 - 3178

Effect of Salinity: The effect of salinity on the photocatalytic degradation efficiency of methylene blue (MB) dye was investigated using the CuS/ZnO nanocomposite photocatalyst, as shown in Fig. 4. The experiments were carried out with an initial MB concentration of 10 ppm, a catalyst dose of 1 g/L, and a pH of 6.5, after 45 minutes of irradiation. The results indicate that salinity levels ranging from 0.25% to 2.50% had minimal impact on the degradation efficiency, with all samples achieving nearly 100% photodegradation. Salinity can influence photocatalytic reactions by introducing ionic species, which may interact with the photocatalyst's surface or reactive intermediates. High salinity levels could potentially inhibit the photocatalytic process due to competition between salt ions and the pollutant for active sites on the photocatalyst surface. However, in this study, the relatively low salinity levels did not significantly affect the degradation efficiency, suggesting that the CuS/ZnO nanocomposite maintains its activity even in saline environments.

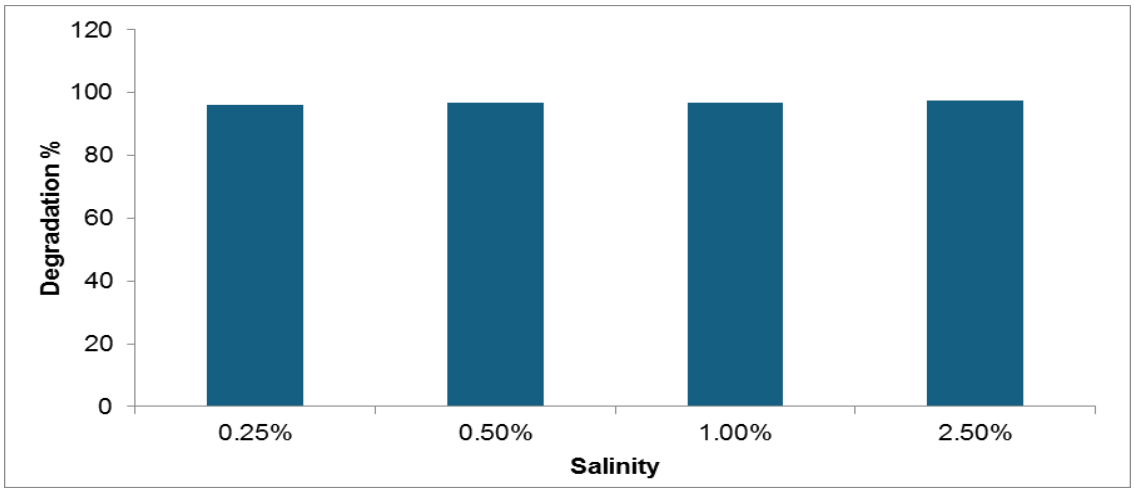

Fig. 4. Effect Salinity on the photocatalytic activity of CuS/ZnO Photocatalyst on the Photodegradation Efficiency MB Dye.

Effect of Scavengers: The effect of various scavenging agents on the photocatalytic degradation efficiency of MB dye was investigated using the CuS/ZnO nanocomposite photocatalyst under simulated sunlight. The experiments were conducted with an initial MB concentration of 10 ppm, a catalyst dose of 1 g/L, and a pH of 6.5, after 45 minutes of

Vol. (54); No. (4); Apr. 2025
Print ISSN 1110-0826
Online ISSN 2636 - 3178

irradiation. Scavengers such as EDTA, ascorbic acid, ethanol, and DMSO were employed to target different reactive oxygen species (ROS), namely holes (h^+), superoxide anion radicals ($O_2^{-\bullet}$), and hydroxyl radicals ($^{\bullet}OH$), as depicted in Fig. 5. The introduction of EDTA, a well-known hole scavenger, enhanced the photocatalytic degradation efficiency to 91% within 15 minutes, When ascorbic acid was used as a scavenger achieving only 65% degradation in the same time frame, Ethanol, although not traditionally used as an active scavenger like EDTA or ascorbic acid, achieved 87% degradation within 15 minutes. Ethanol, although not traditionally used as an active scavenger like EDTA or ascorbic acid, achieved 87% degradation within 15 minutes. the addition of DMSO resulted in a degradation efficiency of 87% within 15 minutes, slightly lower than that observed without scavengers.

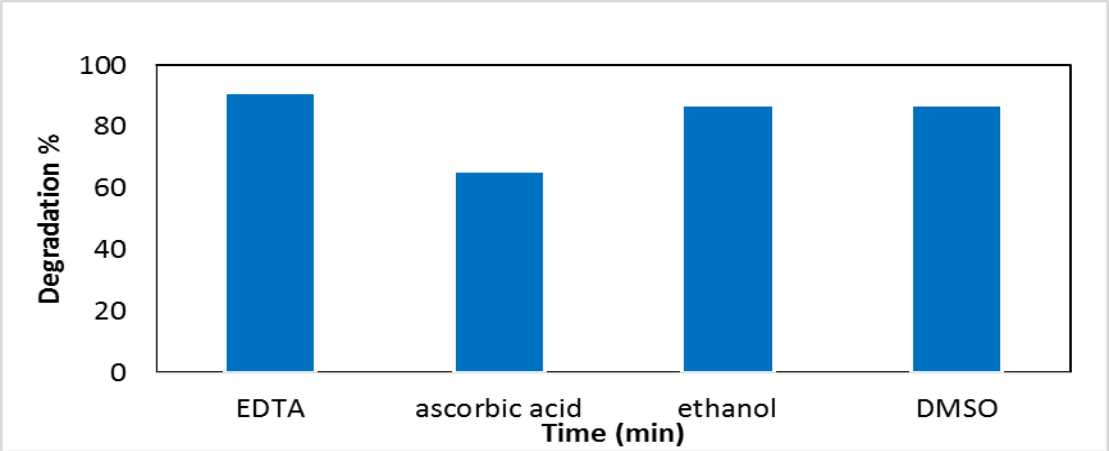

Fig. 5. Effect scavengers on the photocatalytic activity of CuS/ZnO nanocomposite Photocatalyst on the Photodegradation Efficiency MB Dye

Vol. (54); No. (4); Apr. 2025
Print ISSN 1110-0826
Online ISSN 2636 - 3178

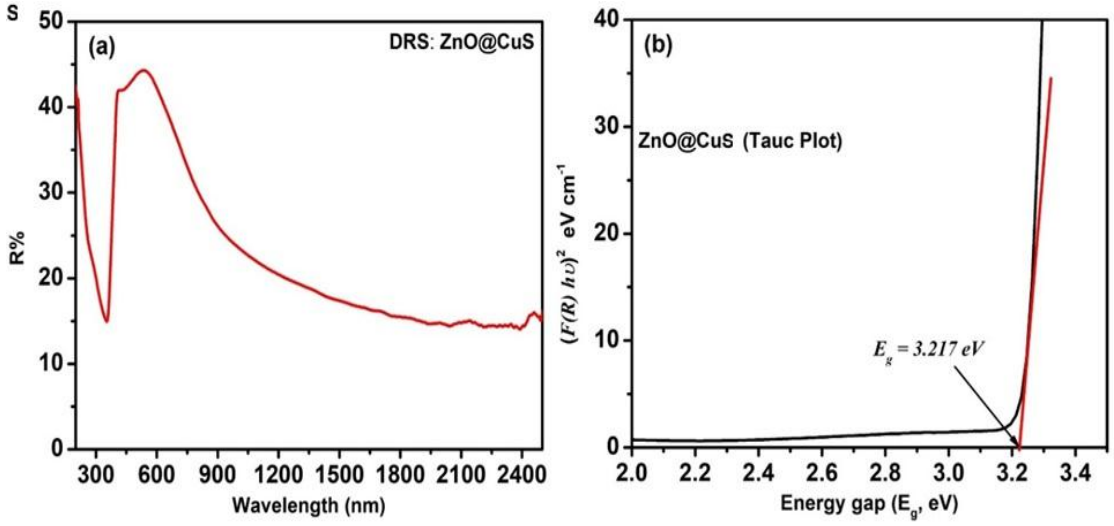

Fig. 6. (a) UV-Vis-NIR diffused reflectance spectrum, and (b) Tauc Plot for estimation of E_g of ZnO/CuS nanocomposites.

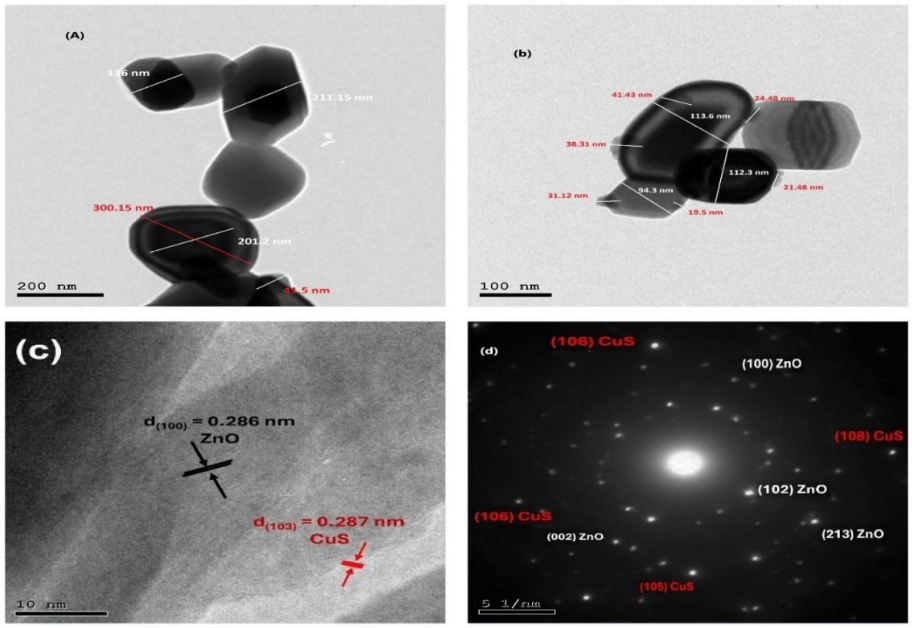

Fig. 7. TEM (a and b), HR-TEM (c) and SAED (d) images of ZnO/CuS nanocomposites

Vol. (54); No. (4); Apr. 2025
Print ISSN 1110-0826
Online ISSN 2636 - 3178

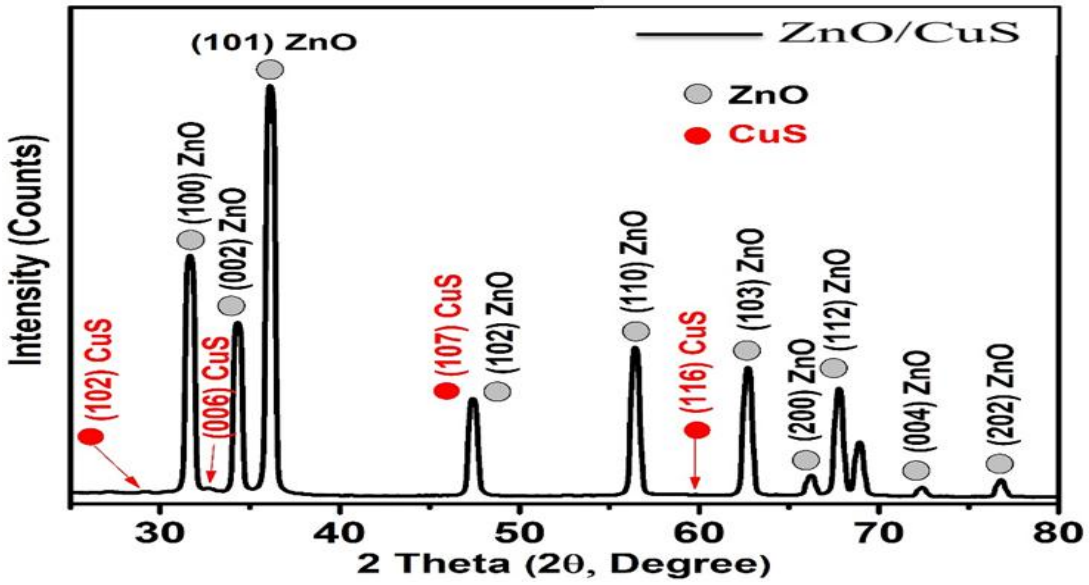

Fig. 8. XRD patterns of ZnO/CuS nanocomposites.

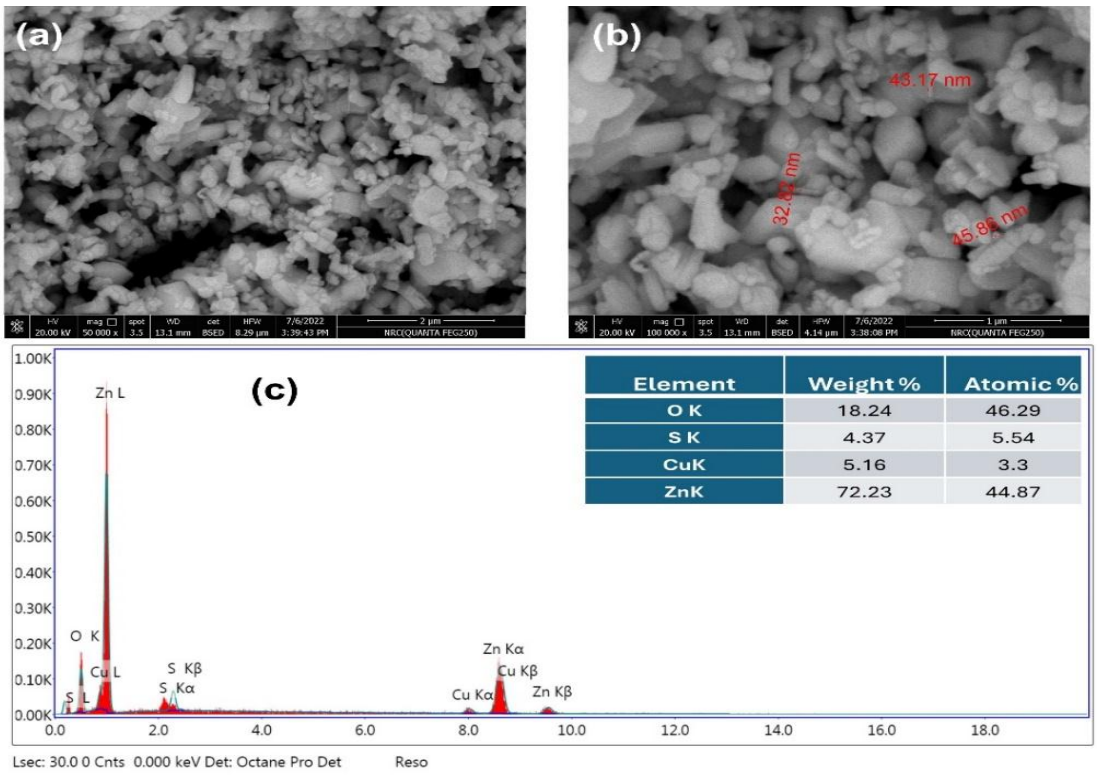

Element	Weight %	Atomic %
O K	18.24	46.29
S K	4.37	5.54
CuK	5.16	3.3
ZnK	72.23	44.87

Fig. 9. SEM images at different magnifications (a and b), and the elemental composition using EDX (c) of ZnO/CuS nanocomposites

Vol. (54); No. (4); Apr. 2025
Print ISSN 1110-0826
Online ISSN 2636 - 3178

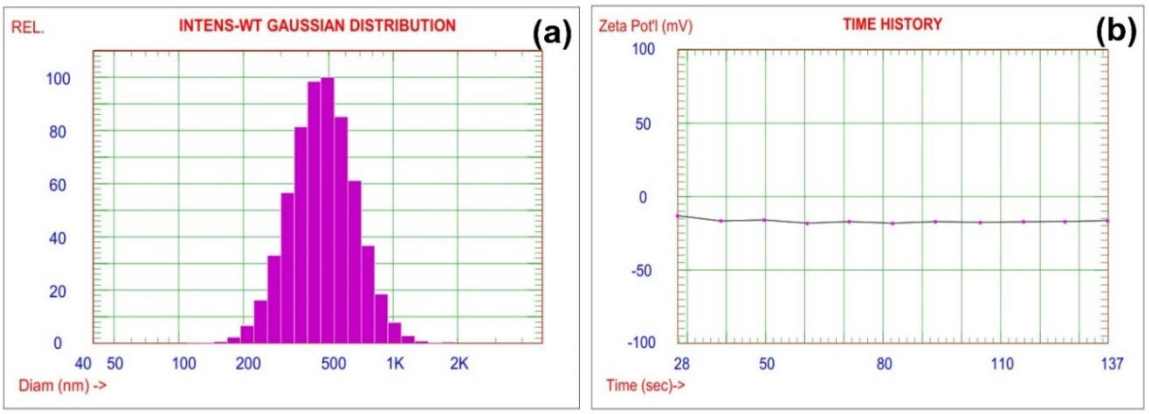

Fig. 10. Colloidal properties including particle size distribution (a) and Zeta potential (b) measurements of ZnO/CuS nanocomposites

Fig. 11. FT-IR spectra of ZnO/CuS nanocomposites

DISCUSSION

The optical properties of ZnO/CuS nanocomposites were investigated using DRS measurements in the UV–Vis–NIR region, as shown in (Fig. 6a). The nanocomposites exhibited significant absorption in the UV and visible light regions, indicating their ability to harvest sunlight effectively. This enhanced absorption is attributed to the synergistic interaction between ZnO and CuS, which broadens the light absorption range compared to the individual components.

Vol. (54); No. (4); Apr. 2025
Print ISSN 1110-0826
Online ISSN 2636 - 3178

The band gap energy (E_g) of the ZnO/CuS nanocomposites was determined using the Kubelka–Munk function and Tauc plot, as shown in Fig. 6b. The relationship is expressed by Eq. (4):

$$F(R) = \frac{K}{S} = \frac{(1-R)^2}{2R} \quad (4)$$

where F(R) is the absorption coefficient, K is the molar absorptivity, S is the scattering factor, and R is the reflectance of the sample, calculated as (R%/100). By extrapolating the linear segment of the $[F(R)h\nu]^2$ vs. hν plot to zero absorption [F(R)=0], the estimated band gap of the ZnO/CuS nanocomposites was found to be approximately 3.217 eV (Fig. 6b). This value is slightly lower than the reported band gap of pristine ZnO nanoparticles (3.29 eV) and higher than the reported band gap of pristine CuS (2.16 eV). The slight reduction in the band gap compared to ZnO is attributed to the coupling effect of CuS, which introduces intermediate energy states that enhance charge transfer and improve the photocatalytic performance under visible light. Meanwhile, the band gap is larger than that of pristine CuS, indicating that ZnO maintains a dominant contribution to the overall electronic structure. This optimized band gap energy ensures efficient utilization of the solar spectrum for photocatalytic applications (**Nandi & Das, 2022**).

The TEM images of the ZnO/CuS nanocomposite provide valuable information about its morphology and structural properties. Fig. 7 (a, b) displays the nanoparticles at different magnifications, revealing a range of particle sizes between approximately 20 nm and 300 nm. The particles exhibit a combination of spherical and irregular shapes, likely due to the co-growth of ZnO and CuS during the synthesis process. This broad size distribution and varied morphology indicates the effective integration of the two components, which is essential for creating a nanocomposite with enhanced functional properties. The ZnO/CuS nanocomposite was characterized by CuS quantum dots (QDs) adhered to or decorating the ZnO NPs, with average particle sizes of 113.4 ± 19.4 nm for ZnO and 29.38 ± 11.2 nm for CuS (Fig. 7b).

Vol. (54); No. (4); Apr. 2025
Print ISSN 1110-0826
Online ISSN 2636 - 3178

It should be noted that the CuS QDs in the composite are consistently within the nanoscale range. This observation aligns with the high-resolution TEM (HR-TEM) results presented in our previous study (Mohammed, R, 2022), which explicitly confirmed the presence of nanoscale CuS quantum dots with well-defined lattice fringes. Although some ZnO/CuS composite particles exceed the nanoscale range, this can be attributed to the agglomeration of smaller particles or secondary growth during the synthesis process. These larger structures do not negate the nanoscale nature of the individual CuS QDs and their role in enhancing the composite's photocatalytic activity.

Further insights into the crystallographic structure were obtained through HR-TEM and selected area electron diffraction (SAED) analysis (Figs. 7c and 7d). The HR-TEM image (Fig. 7c) revealed clear lattice fringes corresponding to two distinct crystallographic planes, confirming the formation of ZnO/CuS heterostructures at the atomic level. The first set of lattice fringes, with an interplanar spacing of 2.87 Å, corresponds to the (103) reflection of the hexagonal CuS structure (ICCD Ref. 00-006-0464). The second set of fringes, with a spacing of 2.86 Å, matches the (100) reflection of the hexagonal ZnO structure (ICCD Ref. 00-036-1451). These results confirm the successful integration of ZnO and CuS phases within the nanocomposites. The close contact between the two phases at the nanoscale level is critical for facilitating efficient charge transfer across the heterojunction, enhancing photocatalytic performance by reducing electron-hole recombination (**Nandi and Das, 2022**). The SAED pattern in panel (D) further confirms the crystalline nature of the ZnO/CuS nanocomposite. Distinct diffraction spots correspond to ZnO (100), (102), (213) and CuS (105), (106), and (108) planes, validating the presence of both components in the hybrid structure. The clear and sharp diffraction spots reflect the high crystallinity of the material, which is essential for its stability and performance in photocatalytic applications (**Urs and Kamble, 2021**).

The crystalline structure of the ZnO/CuS nanocomposite was analyzed using X-ray diffraction (XRD), and the results are presented in the diffraction pattern in Fig. 8. The XRD pattern clearly shows the characteristic peaks of both ZnO and CuS phases, indicating the successful synthesis of the ZnO/CuS nanocomposite (Nandi & Das, 2022; Raj et al., 2020;

Urs & Kamble, 2021), For ZnO, the prominent diffraction peaks observed at 2θ values of approximately 31.8°, 34.4°, 36.2°, 47.5°, 56.6°, 62.9°, and 68.0° correspond to the (100), (002), (101), (102), (110), (103), and (112) planes, respectively, of the hexagonal wurtzite structure (JCPDS No. 36-1451). These peaks confirm the presence of ZnO with high crystallinity in the nanocomposite (Nandi & Das, 2022). For CuS, distinct peaks were detected at 27.8°, 29.2°, 32.9°, 48.0°, 52.7°, and 59.4°, which can be indexed to the (100), (102), (006), (107), (108), and (116) planes, respectively, of the hexagonal covellite structure (JCPDS No. 06-0464). These peaks confirm the successful incorporation of CuS into the composite material. It is important to note that while the CuS peaks may appear less prominent or overlap with the ZnO peaks in some composite samples, the HR-TEM, SAED, and prior studies have clearly verified the existence of CuS quantum dots within the ZnO/CuS nanocomposite. Additionally, the relatively lower intensity of CuS peaks could be attributed to the smaller size of CuS quantum dots and their lower weight fraction in the composite, as well as the strong interfacial interactions between the two phases, which may affect the diffraction intensity of CuS (Raj et al., 2020).

The absence of any additional peaks or impurities in the XRD pattern indicates the high purity of the synthesized ZnO/CuS nanocomposite. Additionally, the presence of both ZnO and CuS peaks suggests strong interfacial contact between the two phases, which is crucial for the heterojunction formation (**Nandi and Das, 2022; Urs** and **Kamble, 2021**). The sharpness and intensity of the diffraction peaks further highlight the high crystallinity of the composite. The integration of CuS with ZnO is expected to enhance the composite's photocatalytic performance due to the effective charge separation facilitated by the heterojunction. These findings are consistent with the TEM and SAED results, which confirm the coexistence of the ZnO and CuS phases with distinct crystallographic interfaces (**Raj et al., 2020**).

The SEM images of the ZnO-CuS nanocomposite at different magnifications are shown in Figures 9 (a) and 9 (b). The micrographs reveal a well-dispersed and interconnected structure with a spherical-like morphology. The average particle size was measured to be in the range of 32.22 nm to 45.98 nm, indicating the formation of nanoscale particles. The

Vol. (54); No. (4); Apr. 2025
Print ISSN 1110-0826
Online ISSN 2636 - 3178

uniform distribution and compact arrangement suggest effective interaction between ZnO and CuS components, which is crucial for achieving enhanced photocatalytic performance.

EDX spectrum and elemental analysis in Fig. 9c displays useful information about the chemical composition of the nanocomposite. The spectrum shows sharp peaks at Zn, O, Cu, and S atoms in the structure, which is indicative of the presence of both ZnO and CuS within this hybrid material. From the elemental composition data, by weight, the most abundant element is zinc, 72.23 %, and equally by atomic percentage, 44.87 %. This means that ZnO is the major constituent of the nanocomposite. The high oxygen content also points towards the presence of ZnO-18.24% by weight (46.29 atom %). The additional presence of copper and sulfur in near stoichiometric proportions of 5.16 wt% and 4.37 wt%, respectively, further confirmed the successful incorporation of CuS into the nanocomposite. The percentage of such elements is relatively lower compared with that of Zn and O; hence, this forms the minor component of the structure.

Furthermore, dynamic light scattering (DLS) and electrophoretic mobility for as-prepared ZnO/CuS nanocomposites in a vehicle solution are represented in Fig 10a and 10b, respectively. The hydrodynamic diameter (H_D) was about 495.7 ± 170.5 nm with a polydispersity index (PDI) of 0.118 (See Fig. 10a), while the zeta potential (η) was about -16.8 mV (See Fig 10b).

The FTIR spectrum of the ZnO/CuS nanocomposite demonstrates distinct transmision bands, confirming the successful synthesis and integration of ZnO and CuS. A broad band observed in the region 3200–3600 cm^{-1} is attributed to the stretching vibrations of hydroxyl groups (-OH). These surface hydroxyls are essential for enhancing the photocatalytic activity of the composite, as they facilitate the trapping of reactive oxygen species during pollutant degradation. The fingerprint region, specifically 500–600 cm^{-1}, reveals peaks corresponding to the stretching vibrations of Zn-O and Cu-O bonds, indicating the presence of ZnO and CuS in the composite. Additionally, the band around 620–650 cm^{-1} is associated with the Cu-S stretching vibrations, further confirming the successful incorporation of CuS into the ZnO matrix. These findings validate the formation of a stable ZnO-CuS nanocomposite **(Malik et al., 2022; Nandi and Das, 2022**). Peaks observed at

2920 cm^{-1} and 2850 cm^{-1} correspond to C-H stretching vibrations, which may originate from organic residues used during the synthesis process. Furthermore, the peaks near 1400–1700 cm^{-1} can be attributed to C=C and N-H stretching vibrations, indicating minor organic impurities or interactions at the composite surface. These groups may also contribute to enhancing the material's photocatalytic properties by influencing surface chemistry.

In the region around 1000–1100 cm^{-1}, bands associated with Zn-OH and Cu-OH bonds are observed. These metal-hydroxyl bonds further emphasize the role of hydroxyl groups in the composite structure. Such functional groups are critical for improving pollutant adsorption and initiating photocatalytic reactions (**Nandi & Das, 2022**).

Photocatalytic Activity Copper Sulfide/Zin Oxide Photocatalyst Nanocomposites

Effect of Photocatalyst Dose

At a dose of **1 g/L**, the photodegradation efficiency reached its maximum, achieving nearly **99% degradation within 45 minutes**. This superior performance can be attributed to the increased availability of active sites and higher surface area, which facilitates the generation of reactive oxygen species (ROS) and improve light absorption. Additionally, the higher catalyst concentration likely promotes better interaction between the dye molecules and the catalyst surface. When the dosage was reduced to **0.5 g/L**, the degradation efficiency decreased to approximately **60% in 45 minutes**. This decline indicates that the number of available active sites becomes a limiting factor at lower catalyst concentrations, resulting in slower degradation rates.

Further reductions in catalyst dosage to **0.4, 0.3, and 0.2 g/L** resulted in progressively lower degradation efficiencies, with minimal activity observed at 0.2 g/L **(Anjum et al., 2023; I. Khan et al., 2022**). The observed trend highlights the critical role of catalyst dosage in determining the photodegradation efficiency of MB dye. Thus, the optimal dose of **1 g/L** demonstrated the highest photocatalytic performance, suggesting its suitability for effective dye removal under simulated solar light irradiation.

Effect of Dye Concentration: Higher efficiencies observed at lower MB concentrations. At 10 ppm, the degradation efficiency reached approximately 98% within 30 minutes, indicating a highly effective photocatalytic process. This superior performance can be

Vol. (54); No. (4); Apr. 2025
Print ISSN 1110-0826
Online ISSN 2636 - 3178

attributed to the availability of sufficient reactive oxygen species (ROS) and active sites on the catalyst surface relative to the lower concentration of dye molecules. As the MB concentration increased to 20 ppm, the degradation efficiency decreased to about 85% in 60 minutes. This reduction suggests that higher dye concentrations impose a competitive scenario, where more MB molecules occupy the active sites, limiting ROS generation and light penetration into the solution (Gong et al., 2017; Gong Cheng et al., 2017; Hu et al., 2019; Mahmoodi, Taghizadeh, Taghizadeh, and Abdi, 2019; Mahmoodi, Taghizadeh, Taghizadeh, and Baglou, 2019; Mahmoodi, Taghizadeh, Taghizadeh, Abdi, et al., 2019; Zhang et al., 2019; Zhang et al., 2015). Further increases in MB concentration to 30 and 40 ppm resulted in significantly reduced degradation efficiencies of around 60% and 40%, respectively, even after 60 minutes. At these higher concentrations, the light absorption by MB molecules competes with the photocatalyst, leading to a reduction in photon energy reaching the catalyst surface. Additionally, the limited availability of active sites and ROS for the excessive dye molecules further diminishes the degradation rate (Reem Mohammed et al., 2022; Mohammed et al., 2023).

Effect of pH: The behavior of MB dye under varying pH conditions is largely governed by its pKa value of 3.8. Above this pH, MB exhibits cationic (positively charged) properties, while below it, the dye assumes anionic (negatively charged) characteristics. Near the pKa value (pH 3.8), molecular interactions with the catalyst surface are minimized, leading to reduced degradation efficiency. At lower pH values (3 and 5), the dye predominantly exists in its ionized state, which impacts surface interactions and reactive species generation, resulting in decreased photocatalytic efficiency at pH 3.

The highest photocatalytic degradation efficiency was observed at pH 9, where an optimal balance between surface charge distribution and chemical conditions was achieved. This facilitated the enhanced production of highly reactive free radicals, leading to superior catalytic performance. Overall, the findings highlight the critical role of pH in optimizing the degradation efficiency of MB dye, with pH 9 emerging as the most favorable condition.

Effect of Salinity : The stability in performance demonstrates the robustness of the CuS/ZnO photocatalyst under saline conditions. The negligible effect of salinity suggests

that the photocatalyst maintains its activity in environments with varying salt concentrations, likely due to its resistance to ion interference during the generation of reactive oxygen species (ROS). These findings underscore the potential applicability of the CuS/ZnO photocatalyst in treating saline wastewater (Wan et al., 2020).

Effect of Scavengers : The effect of various scavenging agents on the photocatalytic degradation efficiency of methylene blue (MB) dye was investigated using the CuS/ZnO nanocomposite photocatalyst under simulated sunlight. Scavengers such as EDTA, ascorbic acid, ethanol, and DMSO were employed to target different reactive oxygen species (ROS), namely holes (h^+), superoxide anion radicals ($O_2^{-\bullet}$), and hydroxyl radicals ($^{\bullet}OH$), as depicted in Fig. 5. The introduction of EDTA, a well-known hole scavenger, enhanced the photocatalytic degradation efficiency to 91% within 15 minutes, indicating that holes (h^+) played a negligible role in the photocatalytic reaction mechanism. When ascorbic acid was used as a scavenger to quench $O_2^{-\bullet}$ radicals, the efficiency decreased significantly, achieving only 65% degradation in the same time frame. This finding highlights the critical contribution of $O_2^{-\bullet}$ radicals to the overall photocatalytic activity. Ethanol, although not traditionally used as an active scavenger like EDTA or ascorbic acid, achieved 87% degradation within 15 minutes. Ethanol can participate in specific chemical reactions involving highly active radicals, particularly in environmental remediation processes. Interestingly, the addition of DMSO resulted in a degradation efficiency of 87% within 15 minutes, slightly lower than that observed without scavengers. This reduction suggests that hydroxyl radicals ($^{\bullet}OH$) are less significant compared to $O_2^{-\bullet}$ radicals in the photocatalytic destruction of MB dye. Overall, the results underline the primary role of $O_2^{-\bullet}$ radicals as the dominant ROS in the photocatalytic process of methylene blue degradation using the CuS/ZnO nanocomposite, with holes and hydroxyl radicals playing secondary roles (Zou et al., 2021).

CONCLUSION AND RECOMMENDATIONS

In this study, ZnO/CuS nanocomposites were successfully synthesized using a microwave-assisted hydrothermal method, demonstrating remarkable potential for

Vol. (54); No. (4); Apr. 2025
Print ISSN 1110-0826
Online ISSN 2636 - 3178

photocatalytic wastewater decontamination. A comprehensive characterization of the material confirmed the integration of ZnO and CuS phases, as evidenced by XRD, TEM, SEM, FTIR, and EDX analyses. The band gap energy of the composite was significantly reduced compared to pristine ZnO, resulting in enhanced absorption in the visible light region and improved photocatalytic efficiency. The photocatalytic degradation of methylene blue dye under simulated solar light highlighted the superior performance of the ZnO/CuS nanocomposite. Optimal operating conditions were identified, including a catalyst dosage of 1 g/L, initial dye concentration of 10 ppm, and pH of 9, under which nearly 100% degradation efficiency was achieved. The effects of varying catalyst dosage, dye concentration, and pH on degradation efficiency were systematically studied, providing critical insights into the operational parameters for practical applications. The results underscore the importance of the synergistic interaction between ZnO and CuS in promoting charge separation and reducing electron-hole recombination, thereby enhancing photocatalytic activity. In conclusion, the ZnO/CuS nanocomposite exhibits excellent photocatalytic properties, making it a promising material for environmental remediation.

REFERENCES

Amar, I. A., Zayid, E. A., Dhikeel, S. A., & Najem, M. Y. (2022). Biosorption removal of methylene blue dye from aqueous solutions using phosphoric acid-treated balanites aegyptiaca seed husks powder. *Biointerface Research in Applied Chemistry*, *12*(6), 7845-7862.

Anjum, F., Shaban, M., Ismail, M., Gul, S., Bakhsh, E. M., Khan, M. A., Sharafat, U., Khan, S. B., & Khan, M. (2023). Novel synthesis of CuO/GO nanocomposites and their photocatalytic potential in the degradation of hazardous industrial effluents. *ACS omega*, *8*(20), 17667-17681.

Barreto, G. P., Morales, G., & Quintanilla, M. L. L. (2013). Microwave assisted synthesis of ZnO nanoparticles: effect of precursor reagents, temperature, irradiation time, and additives on nano- ZnO morphology development. *Journal of Materials*, *2013*(1), 478681.

Basu, M., Garg, N., & Ganguli, A. K. (2014). A type-II semiconductor (ZnO/CuS heterostructure) for visible light photocatalysis. *Journal of Materials Chemistry A*, *2*(20), 7517-7525.

Boudjadar, S., Achour, S., Boukhenoufa, N., & Guerbous, L. (2010). Microwave hydrothermal synthesis and characterization of ZnO nanosheets. *International Journal of Nanoscience*, *9*(06), 585-590.

Capelo-Martınez, J., Ximenez-Embun, P., Madrid, Y., & Cámara, C. (2004). Advanced oxidation processes for sample treatment in atomic spectrometry. *TrAC Trends in Analytical Chemistry*, *23*(4), 331-340.

Crini, G., & Lichtfouse, E. (2019). Advantages and disadvantages of techniques used for wastewater treatment. *Environmental chemistry letters*, *17*, 145-155.

da Costa Filho, B. M., Duarte, A. C., & Rocha-Santos, T. A. (2022). Environmental monitoring approaches for the detection of organic contaminants in marine environments: A critical review. *Trends in Environmental Analytical Chemistry*, *33*, e00154.

Gao, Q., Zhou, L., Xu, S., Dai, S., Zhu, Q., & Li, Y. (2023). Significant improvement and mechanism of tetracycline degradation with the synergistic piezoelectric effect of ZnO/CuS Z-scheme heterojunction photocatalysts. *Environmental Science: Nano*, *10*(2), 581-594.

Gerbreders, V., Krasovska, M., Sledevskis, E., Gerbreders, A., Mihailova, I., Tamanis, E., & Ogurcovs, A. (2020). Hydrothermal synthesis of ZnO nanostructures with controllable morphology change. *CrystEngComm*, *22*(8), 1346-1358.

Ghai, V., Sharma, K., Sanger, J., Singh, H., & Agnihotri, P. K. (2020). Ultrafast microwave-assisted synthesis of various zinc oxide nanostructures. *Indian Journal of Engineering and Materials Sciences (IJEMS)*, *27*(2), 365-372.

Gong, C., Chen, F., Yang, Q., Luo, K., Yao, F., Wang, S., Wang, X., Wu, J., Li, X., & Wang, D. (2017). Heterogeneous activation of peroxymonosulfate by Fe-Co layered doubled hydroxide for efficient catalytic degradation of Rhoadmine B. *Chemical Engineering Journal*, *321*, 222-232.

Gong Cheng, G. C., Chen Fei, C. F., Yang Qi, Y. Q., Luo Kun, L. K., Yao FuBing, Y. F., Wang ShaNa, W. S., Wang XiaoLin, W. X., Wu JiaWei, W. J., Li XiaoMing, L. X., & Wang DongBo, W. D. (2017). Heterogeneous activation of peroxymonosulfate by Fe-Co layered doubled hydroxide for efficient catalytic degradation of Rhoadmine B.

Guo, H.-x., Lin, K.-l., Zheng, Z.-s., Xiao, F.-b., & Li, S.-x. (2012). Sulfanilic acid-modified P25 TiO2 nanoparticles with improved photocatalytic degradation on Congo red under visible light. *Dyes and Pigments*, *92*(3), 1278-1284.

Hezam, A., Namratha, K., Drmosh, Q., Chandrashekar, B. N., Sadasivuni, K. K., Yamani, Z., Cheng, C., & Byrappa, K. (2017). Heterogeneous growth mechanism of ZnO nanostructures and the effects of their morphology on optical and photocatalytic properties. *CrystEngComm*, *19*(24), 3299-3312.

Vol. (54); No. (4); Apr. 2025
Print ISSN 1110-0826
Online ISSN 2636 - 3178

Hoffmann, M. R., Martin, S. T., Choi, W., & Bahnemann, D. W. (1995). Environmental applications of semiconductor photocatalysis. *Chemical reviews*, *95*(1), 69-96.

Hu, L., Zhang, Y., Lu, W., Lu, Y., & Hu, H. (2019). Easily recyclable photocatalyst Bi 2 WO 6/MOF/PVDF composite film for efficient degradation of aqueous refractory organic pollutants under visible-light irradiation. *Journal of Materials Science*, *54*, 6238-6257.

Khader, E. H., Muslim, S. A., Saady, N. M. C., Ali, N. S., Salih, I. K., Mohammed, T. J., Albayati, T. M., & Zendehboudi, S. (2024). Recent advances in photocatalytic advanced oxidation processes for organic compound degradation: A review. *Desalination and Water Treatment*, *318*, 100384.

Khan, I., Saeed, K., Zekker, I., Zhang, B., Hendi, A. H., Ahmad, A., Ahmad, S., Zada, N., Ahmad, H., & Shah, L. A. (2022). Review on methylene blue: Its properties, uses, toxicity and photodegradation. *Water*, *14*(2), 242.

Khan, M. D., Iqra, F., Zulfiqar, A., & Rizwan, M. (2022). Designing of visible light active composites of CuS and ZnO for improved photocatalytic performance under solar light irradiation. *Optik*, *271*, 170147.

Kumar, S. G., & Rao, K. K. (2015). Zinc oxide based photocatalysis: tailoring surface-bulk structure and related interfacial charge carrier dynamics for better environmental applications. *Rsc Advances*, *5*(5), 3306-3351.

Lee, K. M., Lai, C. W., Ngai, K. S., & Juan, J. C. (2016). Recent developments of zinc oxide based photocatalyst in water treatment technology: a review. *Water research*, *88*, 428-448.

Leidinger, P., Dingenouts, N., Popescu, R., Gerthsen, D., & Feldmann, C. (2012). ZnO nanocontainers: structural study and controlled release. *Journal of Materials Chemistry*, *22*(29), 14551-14558.

Lin, M., Chen, H., Zhang, Z., & Wang, X. (2023). Engineering interface structures for heterojunction photocatalysts. *Physical Chemistry Chemical Physics*, *25*(6), 4388-4407.

Low, J., Yu, J., Jaroniec, M., Wageh, S., & Al- Ghamdi, A. A. (2017). Heterojunction photocatalysts. *Advanced materials*, *29*(20), 1601694.

Lu, C., Liu, C., Chen, R., Fang, X., Xu, K., & Meng, D. (2016). Synthesis and characterization of ZnO/ZnS/CuS ternary nanocomposites as high efficient photocatalyst in visible light. *Journal of Materials Science: Materials in Electronics*, *27*, 6947-6954.

Mahmoodi, N. M., Taghizadeh, A., Taghizadeh, M., & Abdi, J. (2019). In situ deposition of Ag/AgCl on the surface of magnetic metal-organic framework nanocomposite and its application for the visible-light photocatalytic degradation of Rhodamine dye. *Journal of hazardous materials*, *378*, 120741.

Mahmoodi, N. M., Taghizadeh, A., Taghizadeh, M., & Baglou, M. A. S. (2019). Surface modified montmorillonite with cationic surfactants: preparation, characterization, and dye adsorption from aqueous solution. *Journal of Environmental Chemical Engineering*, *7*(4), 103243.

Mahmoodi, N. M., Taghizadeh, M., Taghizadeh, A., Abdi, J., Hayati, B., & Shekarchi, A. A. (2019). Bio-based magnetic metal-organic framework nanocomposite: Ultrasound-assisted synthesis and pollutant (heavy metal and dye) removal from aqueous media. *Applied Surface Science*, *480*, 288-299.

Mahpeykar, S., Koohsorkhi, J., & Ghafoori-Fard, H. (2012). Ultra-fast microwave-assisted hydrothermal synthesis of long vertically aligned ZnO nanowires for dye-sensitized solar cell application. *Nanotechnology*, *23*(16), 165602.

Malik, A. Q., Mir, T. u. G., Amin, O., Sathish, M., & Kumar, D. (2022). Synthesis, characterization, photocatalytic effect of CuS-ZnO nanocomposite on photodegradation of Congo red and phenol pollutant. *Inorganic Chemistry Communications*, *143*, 109797.

Mohammed, M., Shitu, A., & Ibrahim, A. (2014). Removal of methylene blue using low cost adsorbent: a review. *Research Journal of Chemical Sciences ISSN*, *2231*, 606X.

Mohammed, R., Ali, M. E. M., Gomaa, E., & Mohsen, M. (2022). Copper sulfide and zinc oxide hybrid nanocomposite for wastewater decontamination of pharmaceuticals and pesticides. *Scientific Reports*, *12*(1), 18153.

Mohammed, R., Ali, M. E. M., Gomaa, E., & Mohsen, M. (2022). Copper sulfide and zinc oxide hybrid nanocomposite for wastewater decontamination of pharmaceuticals and pesticides. *Sci Rep*, *12*(1), 18153.

Mohammed, R., Ali, M. E. M., Gomaa, E., & Mohsen, M. (2023). Promising MoS2–ZnO hybrid nanocomposite photocatalyst for antibiotics, and dyes remediation in wastewater applications. *Environmental Nanotechnology, Monitoring & Management*, *19*, 100772.

Nafees, M., Ali, S., Rasheed, K., & Idrees, S. (2012). The novel and economical way to synthesize CuS nanomaterial of different morphologies by aqueous medium employing microwaves irradiation. *Applied Nanoscience*, *2*, 157-162.

Nandi, P., & Das, D. (2022). ZnO/CdS/CuS heterostructure: A suitable candidate for applications in visible-light photocatalysis. *Journal of Physics and Chemistry of Solids*, *160*, 110344.

Nethravathi, C., Rajamathi, J. T., & Rajamathi, M. (2019). Microwave-assisted synthesis of porous aggregates of CuS nanoparticles for sunlight photocatalysis. *ACS omega*, *4*(3), 4825-4831.

Vol. (54); No. (4); Apr. 2025
Print ISSN 1110-0826
Online ISSN 2636 - 3178

Ning, X., Jia, D., Li, S., Khan, M. F., & Hao, A. (2023). Construction of CuS/ZnO Z-scheme heterojunction as highly efficient piezocatalyst for degradation of organic pollutant and promoting N2 fixation properties. *Ceramics International*, *49*(13), 21658-21666.

Offiong, N.-A. O., Inam, E. J., & Edet, J. B. (2019). Preliminary review of sources, fate, analytical challenges and regulatory status of emerging organic contaminants in aquatic environments in selected African countries. *Chemistry Africa*, *2*, 573-585.

Ozgur, U. (2005). A comprehensive review of ZnO materials and devices. *J. Appl. Phys.*, *98*(41301), 1-103.

Pan, L., Sun, S., Chen, Y., Wang, P., Wang, J., Zhang, X., Zou, J. J., & Wang, Z. L. (2020). Advances in piezo- phototronic effect enhanced photocatalysis and photoelectrocatalysis. *Advanced Energy Materials*, *10*(15), 2000214.

Pang, X., Liu, W., Xu, H., Hong, Q., Cui, P., Huang, W., Qu, Z., & Yan, N. (2022). Selective uptake of gaseous sulfur trioxide and mercury in ZnO-CuS composite at elevated temperatures from SO2-rich flue gas. *Chemical Engineering Journal*, *427*, 132035.

Plumlee, M. H., Larabee, J., & Reinhard, M. (2008). Perfluorochemicals in water reuse. *Chemosphere*, *72*(10), 1541-1547.

Raj, S. I., Jaiswal, A., & Uddin, I. (2020). Ultrasmall aqueous starch-capped CuS quantum dots with tunable localized surface plasmon resonance and composition for the selective and sensitive detection of mercury (ii) ions. *Rsc Advances*, *10*(24), 14050-14059.

Regulacio, M. D., & Han, M.-Y. (2010). Composition-tunable alloyed semiconductor nanocrystals. *Accounts of chemical research*, *43*(5), 621-630.

Santos, C. I., S. Machado, W., Wegner, K. D., Gontijo, L. A., Bettini, J., Schiavon, M. A., Reiss, P., & Aldakov, D. (2020). Hydrothermal synthesis of aqueous-soluble copper indium sulfide nanocrystals and their use in quantum dot sensitized solar cells. *Nanomaterials*, *10*(7), 1252.

Schwarzenbach, R. P., Egli, T., Hofstetter, T. B., Von Gunten, U., & Wehrli, B. (2010). Global water pollution and human health. *Annual review of environment and resources*, *35*(1), 109-136.

Sudhaik, A., Raizada, P., Rangabhashiyam, S., Singh, A., Nguyen, V.-H., Van Le, Q., Khan, A. A. P., Hu, C., Huang, C.-W., & Ahamad, T. (2022). Copper sulfides based photocatalysts for degradation of environmental pollution hazards: A review on the recent catalyst design concepts and future perspectives. *Surfaces and Interfaces*, *33*, 102182.

Sudhaik, A., Raizada, P., Rangabhashiyam, S., Singh, A., Nguyen, V.-H., Van Le, Q., Khan, A. A. P., Hu, C., Huang, C.-W., Ahamad, T., & Singh, P. (2022). Copper sulfides based photocatalysts for degradation of environmental pollution hazards: A review on the recent catalyst design concepts and future perspectives. *Surfaces and Interfaces*, *33*, 102182.

Tadjarodi, A., & Khaledi, D. (2010). Preparation of CuS nanoparticles by microwave irradiation. Proceedings of the 14th International Electronic Conference on Synthetic Organic Chemistry.

Urs, K. M. B., & Kamble, V. (2021). Surface photovoltage response of zinc oxide microrods on prismatic planes: effect of UV, temperature and oxygen ambience. *Journal of Materials Science: Materials in Electronics*, *32*(5), 6414-6424.

Wan, Y., Wan, J., Zhao, J. R., Wang, Y., Luo, T., Yang, S., & Liu, Y. (2020). Facile preparation of iron oxide doped Fe-MOFs-MW as robust peroxydisulfate catalyst for emerging pollutants degradation. *Chemosphere*, *254*, 126798.

Yendrapati, T. P., Gautam, A., Bojja, S., & Pal, U. (2020). Formation of ZnO@CuS nanorods for efficient photocatalytic hydrogen generation. *Solar Energy*, *196*, 540-548.

Zhang, K., Jin, L., Yang, Y., Guo, K., & Hu, F. (2019). Novel method of constructing CdS/ZnS heterojunction for high performance and stable photocatalytic activity. *Journal of Photochemistry and Photobiology A: Chemistry*, *380*, 111859.

Zhang, W., Sun, Y., Xiao, Z., Li, W., Li, B., Huang, X., Liu, X., & Hu, J. (2015). Heterostructures of CuS nanoparticle/ZnO nanorod arrays on carbon fibers with improved visible and solar light photocatalytic properties. *Journal of Materials Chemistry A*, *3*(14), 7304-7313.

Zhao, Y., & Burda, C. (2012). Development of plasmonic semiconductor nanomaterials with copper chalcogenides for a future with sustainable energy materials. *Energy & Environmental Science*, *5*(2), 5564-5576.

Zhao, Y., Pan, H., Lou, Y., Qiu, X., Zhu, J., & Burda, C. (2009). Plasmonic Cu2− x S nanocrystals: optical and structural properties of copper-deficient copper (I) sulfides. *Journal of the American Chemical Society*, *131*(12), 4253-4261.

Zhu, W., Yang, Q., Du, J., Yin, P., Yi, J., Liu, Y., Wu, X., & Zhang, Z. (2022). A Z-scheme CuO–ZnO–ZnS–CuS quaternary nanocomposite for solar-light-driven photocatalytic performance. *Current Applied Physics*, *39*, 113-121.

Zou, R., Li, L., Yang, L., Lan, J., Liu, H., Dou, B., Shang, J., & Lin, S. (2021). CeO 2/CdS heterojunction decorated cotton fabric as a recyclable photocatalyst for efficient light driven degradation of methylene blue. *Cellulose*, *28*, 11081-11096.

Vol. (54); No. (4); Apr. 2025
Print ISSN 1110-0826
Online ISSN 2636 - 3178

Journal of Environmental Sciences (JES)
Faculty of Graduate Studies and Environmental Research, Ain Shams University

تحضير وتوصيف متراكبات نانوية من أكسيد الزنك وكبريتيد النحاس لتنقية المخلفات العضوية للمياه باستخدام التحفيز الضوئي.

أحمد فوزي[1]– ريم محمد[2]– هاني العزب[3]– محمد عيد محمد علي[4]– مني محسن[2]

1) كلية الدراسات العليا والبحوث البيئية، جامعة عين شمس، القاهرة، مصر 2) قسم الفيزياء، كلية العلوم، جامعة عين شمس، القاهرة، مصر 3) قسم الهندسة الكيميائية والكيميائية الحيوية، جامعة ميسوري للعلوم والتكنولوجيا، رولا، ميسوري 65409، الولايات المتحدة الأمريكية 4) قسم أبحاث تلوث المياه، المركز القومي للبحوث، القاهرة، مصر

المستخلص

تقدم هذه الدراسة تخليق وتوصيف مركبات نانوية هجينة من أكسيد الزنك/ كبريت النحاس مصممة للتحلل الضوئي لصبغة الميثيلين الأزرق. تم تصنيع المركبات النانوية باستخدام طريقة حرارية مائية بمساعدة الميكروويف، حيث تم تحضير كبريتيد النحاس(CuS) أولاً، تم بعد ذلك إضافة جسيمات نانوية من أكسيد الزنك (ZnO NPs). تم تأكيد التكامل الناجح بين كبريتيد النحاس وأكسيد الزنك باستخدام تقنيات توصيف مختلفة، بما في ذلك حيود الأشعة السينية (XRD)، والمجهر الإلكتروني النافذ (TEM)، والمجهر الإلكتروني الماسح (SEM)، وطيف الأشعة السينية المشتتة للطاقة (EDX)، وطيف الأشعة تحت الحمراء بتحويل فورييه (FTIR)، كما تم التحقيق في الخصائص البصرية باستخدام مطيافية الانعكاس المنتشر (DRS)، وكشفت أن طاقة الفجوة النطاقية للمادة الهجينة (3.21 إلكترون فولت) كانت أقل من طاقة أكسيد الزنك النقي (3.29 إلكترون فولت)، مما يشير إلى زيادة النشاط الضوئي التحفيزي. أثبتت تجارب التحلل الضوئي كفاءة عالية في إزالة اللون الأزرق الميثيليني، مع تحقيق تحلل الصبغة بالكامل في ظل الظروف المثلى: جرعة المحفز الضوئي 0.1 جم / لتر، وتركيز الصبغة 10 جزء في المليون، ودرجة حموضة 9. تسلط هذه النتائج الضوء على إمكانات متراكبات النانو ZnO / CuS للتطبيقات العملية في معالجة مياه الصرف الصحي. علاوة على ذلك، تم التحقيق بشكل منهجي في تأثير الملوحة والأيونات الأكسجينية غير العضوية وكاسحات النفايات على الأداء التحفيزي الضوئي، مما يوفر رؤى مهمة في المعلمات التشغيلية المطلوبة لاستخدام متراكبات النانو ZnO / CuS في معالجة البيئة بشكل فعال.

الكلمات المفتاحية: الميكروويف، الطاقة الحرارية المائية؛ مياه الصرف الصحي؛ أكسيد الزنك؛ كبريتيد النحاس؛ التحفيز الضوئي.

Vol. (54); No. (4); Apr. 2025
Print ISSN 1110-0826
Online ISSN 2636 - 3178